Profiling of barrier capacitance and spreading resistance using a transient linearly increasing voltage technique

E. Gaubas,[a] T. Čeponis, and J. Kusakovskij
Vilnius University, Institute of Applied Research, Sauletekio av. 9-III, LT-10222 Vilnius, Lithuania

(Received 31 March 2011; accepted 1 August 2011; published online 24 August 2011)

A technique for the combined measurement of barrier capacitance and spreading resistance profiles using a linearly increasing voltage pulse is presented. The technique is based on the measurement and analysis of current transients, due to the barrier and diffusion capacitance, and the spreading resistance, between a needle probe and sample. To control the impact of deep traps in the barrier capacitance, a steady state bias illumination with infrared light was employed. Measurements of the spreading resistance and barrier capacitance profiles using a stepwise positioned probe on cross sectioned silicon pin diodes and pnp structures are presented. © *2011 American Institute of Physics*. [doi:10.1063/1.3626796]

I. INTRODUCTION

Several techniques are commonly employed in profiling the chemical structure of materials, such as secondary ion mass spectroscopy,[1] and the distribution of electrically active dopants and carrier density, such as scanning spreading resistance microscopy (SSRM), and scanning capacitance microscopy (SCM).[2] The latter SCM technique[2] is based on small ac test signal phase shift measurements due to the barrier capacitance between a probe-tip and the material under investigation. The SSRM and SCM methods are well standardized for scanning microscopy with a spatial resolution approaching a few nanometers.[3] However, doping and steady-state carrier density profiles can be insufficient to predict the operational characteristics of fabricated junctions if additional defects are introduced together with the dopants.

The technique employed in this work for the simultaneous control of the barrier capacitance, using interior junctions of layered (inhomogeneous) structures, and the spreading resistance (at the probe-tip), enables the highlighting of the depleted interfaces, which are hidden when simple scanning of the spreading resistance is applied to profiling.[3,4] In this work, this technique for barrier evaluation using a linearly increasing voltage (BELIV) is presented based on measurements of the current transients at the reverse and forward pulsed bias. The spreading current pulsed measurements are performed when a plate electrode and a probe-tip are linked to the same material layer within the profiling area. This barrier control technique is combined with a step-positioning of the needle-tip probe, located on the cross sectional boundary of a parallel-plate layered structure, which enables simultaneous control of the spreading resistance, barrier capacitance, and parameters of the deep traps.

II. EXPERIMENTAL ARRANGEMENT

A sketch of a simple measurement circuitry for implementation of BELIV profiling is illustrated in Fig. 1(a). Current transients have been recorded using the 50 **Ω** load input of an oscilloscope. Additionally, the measurement circuitry contains the adjusted output of a generator of linearly increasing voltage (LIV) and the junction structure under investigation, connected in series. The cross sectional boundary of a layered junction structure is scanned by a gold needle positioned by a precise 3D stepper. The micro-structure of the needle-tip (making a slightly non-ohmic electrical contact) determines the appearance of the spreading currents between the main plate electrode (a deposited metal layer) of a relatively large area and the needle tip on the boundary of a structure located (perpendicularly to the main electrode) within a definite layer and at a point of definite depth. The electrical contact between the needle-tip probe and sample is controlled by reaching the maximum current and manipulated by pressing the needle probe. The position of the probe on the boundary is changed by pull-shift-press procedures in sequence using a 3D stage and keeping a fixed pressure on the probe. The boundary of the samples for depth profiling was carefully prepared to be as smooth as possible. The needle-tip was sharpened by mechanical and chemical procedures. A complementary continuous-wave infrared (IR) light source, either a laser with wavelengths in the range of 1–5 μm or a photometric 350 W lamp, is employed to vary the filling of the deep centers.

III. PRINCIPLES OF EXTRACTION OF PARAMETERS

The application of the BELIV technique to a reverse biased diode containing an abrupt junction is based on the analysis of barrier capacitance (C_b) changes with a linearly increasing voltage $U_P(t) = At$ pulse. The $C_b(t)$ dependence on voltage and thereby on time t can be described using the depletion approximation[5] for charge extraction in the trap-free material. This approximation leads to a simple relationship $C_b = C_{b0}(1+U/U_{bi})^{-1/2}$ for an abrupt p^+-n junction, where the barrier capacitance of the non-biased diode of an area S is given by $C_{b0} = \varepsilon\varepsilon_0 S/w_0 = (\varepsilon\varepsilon_0 S^2 eN_D/2U_{bi})^{1/2}$. Here ε_0 is the vacuum permittivity, ε is the material dielectric permittivity, e is the elementary charge, U_{bi} is the built-in

[a]Author to whom correspondence should be addressed. Electronic mail: eugenijus.gaubas@ff.vu.lt.

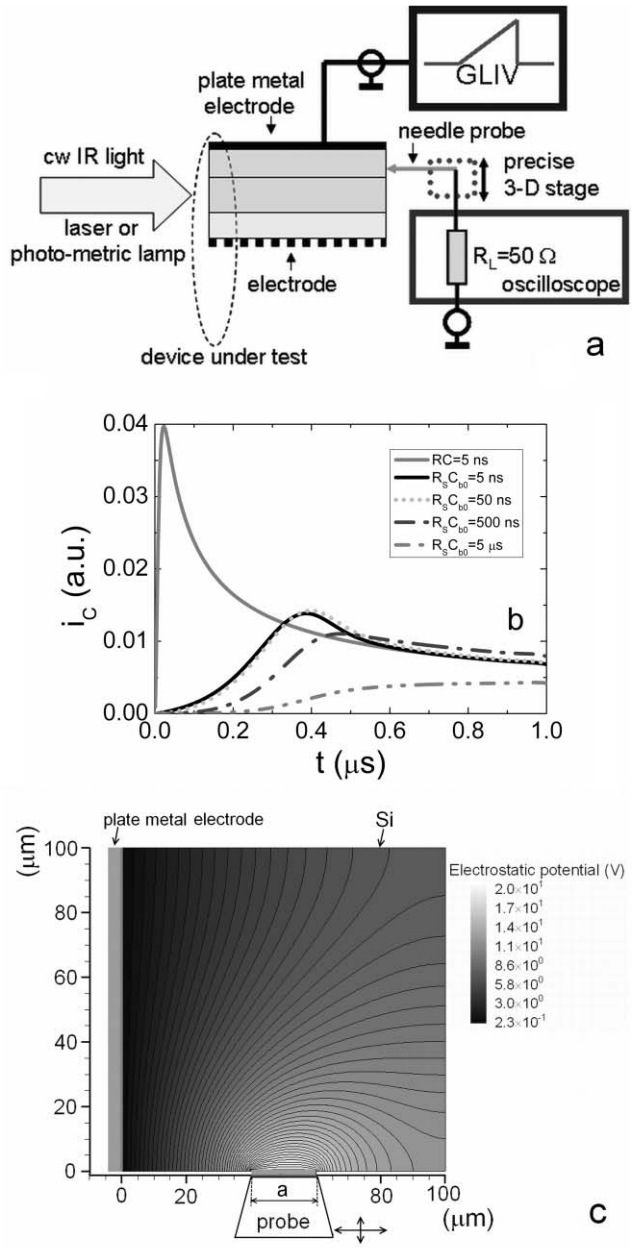

FIG. 1. (a) Sketch of the measurement circuitry for the implementation of BELIV profiling. A continuous-wave infrared (IR) light source (LS) is used to vary the filling of deep centers. (b) Simulated reverse biased BELIV current $i_C(t)$ for the parallel-plate electrodes and for an initial delay $RC = 5$ ns (solid grey curve) compared with those obtained for a boundary probe located within a high resistivity material layer behind the interface of an abrupt junction, whereby the delay R_SC_{b0} (broken and black curves) is dependent on the spreading resistance R_S. The broken and black (solid) curves illustrate the simulated transients for a BELIV response measured on $R_L = 50\ \Omega$ using a convolution integral with R_SC_{b0} values of $R_SC_{b0} = 5$ ns (black solid), 50 ns (dotted), 500 ns (dashed-dotted), and 5 μs (grey dashed-dotted-dotted), respectively. (c) Simulated distribution of the potential (using the TCAD platform, Alternative Solutions) within a single layer for the perpendicularly located probes in different areas. Values of the potential are indicated by a white-grey-black bar.

potential barrier, N_D is the doping density, $w_0 = (2\varepsilon\varepsilon_0 U_{bi}/eN_D)^{1/2}$ the width of the depletion of the non-biased junction and $A = U_P/\tau_{PL}$ is the ramp of the LIV pulse of the U_P amplitude and the τ_{PL} duration. The time dependent changes of charge $q = C_bU$ within a junction determine the current transient $i_C(t) = AC_{b0}[1 + (At/2U_{bi})][1 + (At/U_{bi})]^{-3/2}$ in the external circuit. These transients contain an initial ($t = 0$) step AC_{b0} due to the displacement current and a descending constituent governed by charge extraction. A delay appears due to the serial processes of dielectric relaxation, drift, and diffusion of carriers to complete the circuit. The characteristic lifetimes of these processes together with the serial spreading resistance, summarized as τ_{RC}, lead to a delay. Hence the RC_{b0} modified transients can be roughly emulated by the convolution integral $i_{RC}(t) = (1/\tau_{RC})\int_0^t i_C(x)\exp[-(t - x)/\tau_{RC}]dx$. The simulated currents, including τ_{RC}, are illustrated in Fig. 1(b). It is worth noting that, for a pure capacitor within an RC circuit, the voltage transient measured on the load resistor exhibits a square-wave shape when using a LIV pulse. For the precise description of the BELIV transient of large C_{b0} and $i_C(t)$, the nonlinear differential equation $(dU_C/dt)[1 + (U_C(t)/2U_{bi})] \times [1 + (U_C(t)/U_{bi})]^{-3/2} - [(U_P(t) - U_C(t))/\mathrm{RC}_{b0}] = 0$ should be numerically solved, including the nonlinear voltage sharing between the load resistor and the junction structure. The simultaneous action of different traps, through the emission of carriers (with a generation lifetime τ_g), can be observed in the BELIV response via the collection of charge generated within the depleted region. This space charge generation current, expressed as $i_g(t) = (en_iSw_0/\tau_g)[1 + (U_C(t)/U_{bi})]^{1/2}$, increases with the voltage $U_C(t)$. The current $i_g(t)$ can exceed the barrier charging current $i_C(t)$ in the rearward range of the pulsed (BELIV) transient. The transient of the total reverse current ($i_{R\Sigma}$) is then described by the sum of the $i_C(t)$ and $i_g(t)$ constituents. The descending charge extraction and the ascending generation current variation with the LIV pulse time (voltage) implies the existence of a current minimum within a transient. The simulated transient of the charge collection regime is illustrated in Fig. 1(b). The BELIV current $i_{\Sigma F}(t)$ transients and their analysis become more complicated with the forward LIV biasing of the diode. Generally, the $i_{\Sigma F}(t)$ current appears to be composed of the barrier ($i_{CF}(t)$) and diffusion (storage) capacitance charging ($i_{Cdiff}(t)$) currents and of the recombination ($i_R(t)$) and injection ($i_{injcF}(t)$) currents. The storage capacitance is routinely assumed to be $C_{diff}(t) = d(\int_0^t i_{diff0}(\exp(eU(t')/k_BT) - 1)dt')/dU$. At forward biased LIV, the initial stages of the BELIV transient are governed by the barrier capacitance current $i_{CF}(t) = (dU_F/dt)C_{b0}[1 - (U_F(t)/2U_{bi})][1 - (U_F(t)/U_{bi})]^{-3/2}$, which slowly increases with $U_F(t)$. At $t \cong 0$ the diffusion capacitance and current are close to zero. Thus, for the low injection level regime, the barrier capacitance component prevails over both the diffusion and recombination current components during the initial stages of the current transient at forward biasing. The amplitude of the BELIV current during the ulterior phase of the BELIV transient, exponentially increases due to $i_{Cdif}(t) = (dU_F/dt)C_{diff0}\{\exp(eU_F(t)/k_BT)[(eU_F(t)/k_BT) + 1] - 1\}$. Here, $C_{diff0} = i_{diff0}/(dU/dt) \cong i_{diff0}/A$ and k_BT is the thermal energy. For a quantitative estimation of the barrier characteristics, a combined analysis of the height of the initial step of current for the reverse $i_{R\Sigma}(0) \approx AC_{b0} + i_g$ and forward $i_{\Sigma F}(0) = AC_{b0} + (en_iSw_0/2\tau_R)$ biased diode is performed.

IV. PROFILING OF LAYERED STRUCTURES

For electrodes of the perpendicular configuration, when a needle-tip is positioned on the cross sectional boundary of a parallel-plate layered structure, the current spreading effect should be included. The spreading of current in a material of resistivity ρ acts as a serial resistance $R_S = \rho l_{eff}/S_{eff}$ introduced into the BELIV measurement circuit. The latter is very sensitive to R_S changes. The simulated distribution of potential (using TCAD software for specific configuration of the probes) is illustrated in Fig. 1(c). For high symmetry of the measurement configuration, as in common spreading resistance measurements, the approximation $l_{eff}/S_{eff} = 1/2a$ can be used. In fact, the low symmetry of the geometrical configuration used in the present study does not allow simplifications. Therefore, complicated numerical simulations (starting from the solution of the Poisson equation) are inevitable when modeling the changes of the transients during profiling. It can be noted in Fig. 1(c) that the concentration of the electric field and consequently of the current density is significantly enhanced at the beginning (edges) of the probe. Thus, the spatial resolution of profiling can be higher than that evaluated using the diameter (a) of the needle-probe. To evaluate the ratio of l_{eff}/S_{eff} and the absolute values of R_S and N_D, a calibration procedure should be used which can be performed by varying U_P, τ_{PL}, R_L and using a set of material samples combined with a definite probe system.

The industrial, rather perfect pin diode structures with well-defined layer widths and doping densities, were used for testing the BELIV profiling technique. The specific variation of the BELIV transients is illustrated in Fig. 2(a). Profiles of the peak amplitudes and the durations of the BELIV pulse τ_{BELIV} are shown in Fig. 2(b). τ_{BELIV} is the time interval between the barrier charging current peak and the end of the LIV pulse whereby these particular points can be distinguished precisely. For locations of a Au probe within a cross sectional boundary (shifting the probe by a 3D stage) in the vicinity of the metallic plate electrode and high conductivity emitter (p^+) layer, the amplitude and shape of the BELIV transient are close to that of the LIV pulse [Fig. 2(a)]. The decrease of the peak amplitude for probe locations within a relatively high resistivity layer is determined by the spreading resistance (due to the needle-tip probe). Thus, the BELIV transient is governed by the main junction of the diode under investigation. The shape of the registered transient is inherent for the diode, which is reverse biased by the LIV pulse, in this case. A rise in this current is then either significantly stretched within the initial front of the BELIV pulse or even shifted over the time scale [Fig. 2(a), curves for the location of the probe at 50 and 100 μm] causing a shortening of τ_{BELIV}. An increment of $R_S C_{b0}$ induces a shift of the current peak (AC_{b0}) toward the longer time scale relative to the beginning of τ_{PL} and to the initial step of dU_P/dt for the LIV pulse.

The amplitude and duration of the BELIV transient (τ_{BELIV}) are restored [Fig. 2(b)] by moving the probe from the highest resistance (n-base) region toward the enhanced conductivity layer (n^+). The regeneration of the amplitude and the reduction of the delay for transients registered behind the n/n^+ interface are caused by the decrease of the resistivity

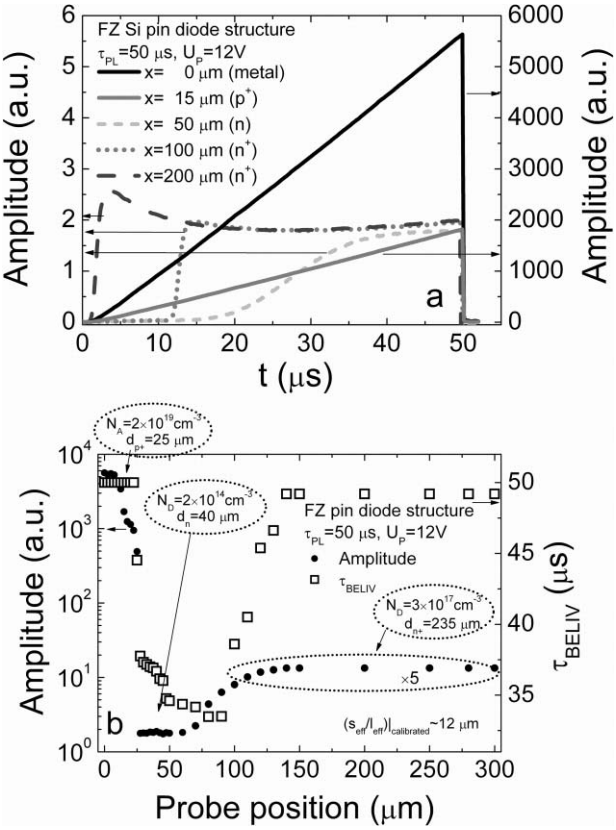

FIG. 2. (a) Variations of the BELIV transients in a p^+nn^+ structure of a pin diode for a probe positioned (x) within different layers. (b) Variations of the amplitude and the BELIV pulse duration, obtained by depth-scans of the p^+nn^+ structure.

within the n^+ layer and the decrement of R_S. Nearly the whole n/n^+ interface then acts as another parallel-plate electrode leading to an increased effective area. The range of the inherent changes in the BELIV transient (for both the amplitude and τ_{BELIV}) clearly indicates the geometrical dimension of the layer of highest resistivity over the structure, Fig. 2(b). Fitting the simulated characteristics to the experimental data enables the extraction of the parameters of spreading resistance and barrier parameters. The measured profile of the BELIV amplitudes [Fig. 2(b)] has been compared with doping profiles obtained using common spreading resistance scans performed by a commercial R_S profiler on the same types of structure. The width of the outspread of amplitude variations within the interfacial regions between p^+/n and n/n^+ layers and the doping densities have been found to be in excellent agreement with those obtained by common R_S scans.

The crucial impact of impurity induced deep centers on the BELIV profiling has been found within pnp structures and on commercial (n^+pnp) thyristor structures. Therefore, the BELIV technique has been applied in this case using, in addition, steady-state infrared bias illumination (BI). For layers containing a high density of traps, the BELIV transient [illustrated in Fig. 3(a)] recorded for a single scan point contains an initial recess. The latter indicates a reduced AC_{b0} barrier charging current due to traps filling if the density of the BI is insufficient. This impact of traps can be highlighted or suppressed by the enhancement of the steady-state

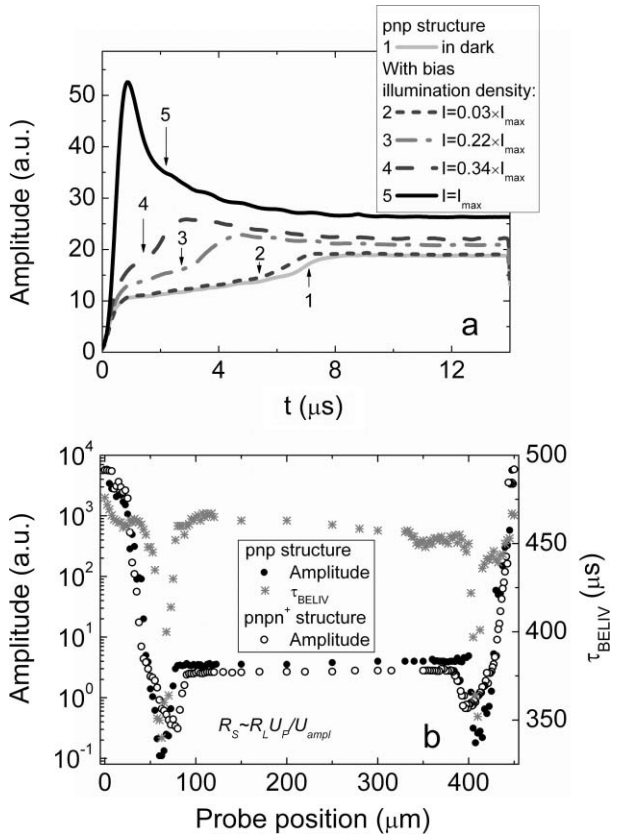

FIG. 3. (a) Bias illumination (BI) density dependent charge extraction current transients measured at a fixed position of the needle probe (within the n-type bulk of the pnp structure) for the same reverse (U_R) voltage of LIV pulses. (b) Comparison of the amplitude (black solid symbols) and τ_{BELIV} (grey stars) profiles for pnp (solid symbols) and completed thyristor (open symbols) structures.

BI density. The initial recess in the BELIV transient disappears with increasing IR light density. Figure 3 shows the result when carrier capture centers are filled and a recombination current is reduced. The profiles of the amplitude of the BELIV response (measured with proper BI) obtained for pnp and n^+pnp structures are illustrated in Fig. 3(b). These scanned profiles are associated with the extent (spatial dimension) of the doped layers and of the interfaces (pn and np) between them. The drop in the BELIV amplitude, obtained going from a p- to an n-layer, represents a change in doping from 10^{17} to 10^{13} cm^{-3}.

V. SUMMARY

In summary, the BELIV technique presented is a tool for the fast estimation of the actual location of barriers (depleted regions), of doping profiles, and of deep traps within the layered junction structures. A profile of amplitudes of a spreading current pulse (which repeats the shape of a LIV pulse) is recorded when both a plate electrode and a probe-tip are linked to the same conductivity-type material layer. This segment of a scan of the layered structure provides a spreading resistance (doping density) profile. The current transient changes its shape from LIV-like to that inherent for a barrier capacitance charging current when a probe-tip crosses a metallurgic boundary between the layers of opposite conductivity type. Combined analysis of the amplitude and the BELIV pulse duration provides parameters for the spreading resistance in the second layer and for the effective doping density ascribed to the depleted width for the junction under test. The calibrated spectrum and intensity of bias illumination, sufficient to suppress carrier capture centers, enable the evaluation of the density of these centers and the estimation of the carrier capture lifetimes. Control of the carrier thermal emission (space charge generation) current component allows the estimation of carrier emission lifetimes when the latter fit a LIV pulse time scale. Switchover of the applied voltage polarity and a consequent change of shape of the BELIV transient provide information about the conductivity-type of the layers under test. The current of the forward biased junction (within ulterior stage of the BELIV pulse) can be a measure of barrier injection capability and carrier recombination lifetime. This technique has been applied and is shown to be suitable for the examination of particle detector, pin-diode, thyristor, and solar–cell structures. Depth variations of the amplitude, of the shape, and of the duration of the BELIV transients are in good agreement with the same characteristics evaluated using common R_S profiling instruments, while extracted parameters of C_b and τ_g correlate well with those determined using the DLTS (deep level transient spectroscopy) technique on the same samples.

ACKNOWLEDGMENTS

This work was supported by the Lithuanian Science Council Grant MIP-11018.

[1]J. C. Vickerman and I. S. Gilmore, *Surface Analysis – The Principal Techniques*, 2nd ed. (Wiley, Chichester, 2009).
[2]S. Kalinin and A. Gruverman, *Scanning Probe Microscopy* (Springer, New York, 2007), Vol. 1.
[3]X. Ou, P. Das Kanungo, R. Kogler, P. Werner, U. Gosele, W. Skorupa, and X. Wang, Nano Lett. **10**, 171 (2010).
[4]D. K. Schroder, *Semiconductor Material and Device Characterization*, 3rd ed. (Wiley, New Jersey, 2006).
[5]P. Blood and J. W. Orton, *The Electrical Characterization of Semiconductors: Majority Carriers and Electron States* (Academic, London, 1992).